ACS Sustainable Chemistry & Engineering

Research Article

pubs.acs.org/journal/ascecg

Green Synthesis of a Gold Nanoparticle–Nanocluster Composite Nanostructures Using Trypsin as Linking and Reducing Agents

Longhua Zou,[†] Wei Qi,[†] Renliang Huang,*[,‡] Rongxin Su,*[,†] Mengfan Wang,[†] and Zhimin He[†]

[†]Synergetic Innovation Center of Chemical Science and Engineering (Tianjin), State Key Laboratory of Chemical Engineering, School of Chemical Engineering and Technology, Tianjin University, Tianjin 300072, PR China

[‡]School of Environmental Science and Engineering, Tianjin University, Tianjin 300072, PR China

Supporting Information

ABSTRACT: We report a green synthesis of novel gold nanoparticle–nanocluster composite nanostructures directly using trypsin as linking and reducing agents. Size exclusion chromatography (SEC) and transmission electron microscopy (TEM) reveals that the as-prepared gold nanocomposite (gold nanoparticles-trypsins-nanoclusters, GNPs-Trys-GNCs) is composed of GNPs (gold nanoparticles) with an average diameter of 5.5 nm and the GNCs (gold nanoclusters, about 1 nm)-embedded trypsins (Trys-GNCs), which are attached to the surface of the GNPs. The specific amino acids in the trypsin molecule, like cysteine, methionine, and tyrosine, combined with the unique spatial structures, enable trypsins to bind and reduce the $AuCl_4^-$ ions, simultaneously forming GNPs and GNCs in one-pot synthesis. Similar to pure GNPs, the GNPs-Trys-GNCs nanocomposite also exhibits an intense surface plasmon resonance (SPR) absorbance at 520 nm. However, it shows an obvious different optical property in the interaction with Pb^{2+} ions. In the presence of Pb^{2+} ions, an increased intensity and a slight red-shift of the SPR peak for the GNPs-Trys-GNCs nanocomposite in the UV–vis spectra were observed, while a decreased intensity and large red-shift for pure GNPs were observed in previous studies. Moreover, we found that the SPR intensity linearly increased with Pb^{2+} concentration from 1.6 to 32.3 μM (R^2 = 0.9731). In addition, high-level Pb^{2+} ions would induce the aggregation of GNPs-Trys-GNCs nanocomposite accompanied by the formation of precipitate. The unique structure and optical property of the GNPs-Trys-GNCs nanocomposite enable it to be used in heavy metal ions sensing and elimination.

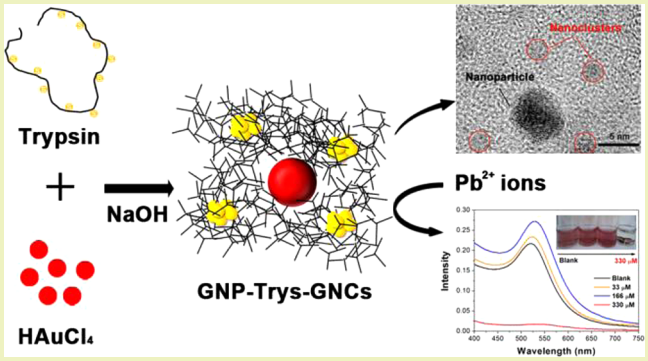

KEYWORDS: *Gold nanoparticles, Gold nanoclusters, Protein template, Biomineralization, Nanostructure, Nanocomposite*

INTRODUCTION

Gold nanoparticles (GNPs) are some of the most extensively studied nanomaterials in recent years due to their charming optical, chemical, and physical properties. Particularly, accurately controlling the microstructure such as shape, size, and composition of GNPs opens an important avenue for revealing their new or enhanced functions in various applications, such as biomedicine, biosensor, organic photovoltaics, and some other areas.[1] Recent advances have emerged a new class of quantized fluorescent GNPs that consist of several to dozens of gold atoms with a diameter of ~1 nm.[2−4] To differentiate conventional plasmonic GNPs, these ultra-small GNPs are specially denoted as gold nanoclusters (GNCs).[5] In contrast with quasi-continuous electronic bands of GNPs (>5 nm), GNCs have discrete energy levels, leading to their unique fluorescence, chiral, and magnetic properties. High quantum yield, good biocompatibility, and stability against photobleaching render GNCs an excellent candidate for bioimaging, cell targeting, and biomedical engineering.[6,7]

To improve the application performance of gold nanoparticles, especially in biomedicine and biosensors, some biomacromolecules like peptides, proteins, enzymes, antibodies, and DNA were often used to functionalize them through covalent or noncovalent conjugation.[8,9] Inspired by the highly ordered architecture and precise molecular recognition of these biomolecules, in addition to the biomolecule-modified GNPs via post-functionalization, many researchers had focused on the synthesis of gold nanomaterials directly using biomolecules as the stabilizing and reducing agents. Take peptides and proteins for example, these molecules contain amino acid residues with reducing ability, like tyrosine and cysteine,[10,11] which are capable of reducing chloroauric acid rapidly under mild conditions. Shao et al.[12] had demonstrated the roles of specific-binding amino acid (e.g., aspartate, tryptophan, tyrosine) in construction of gold nanostructures. On the basis of these specific-binding amino acids, some peptide ligands, such as PEP_{Au} (AYSSGAPPMPPF)[13,14] and AG4 (NPSSLFRYLPSD),[15] were designed and used to direct the synthesis of gold nanoparticles, further controlling the assembly

Received: May 7, 2013
Published: August 17, 2013

 © 2013 American Chemical Society

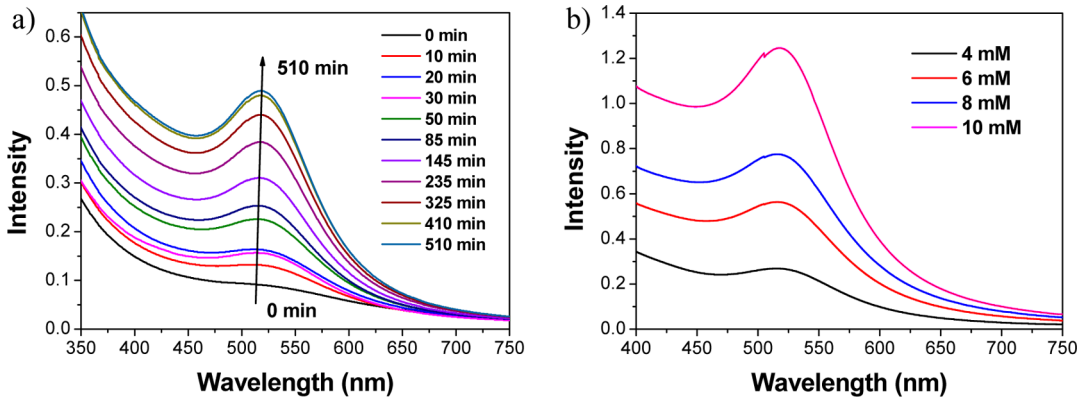

Figure 1. UV−vis spectra of as-prepared samples with increasing time (a) and with increasing $HAuCl_4$ concentrations (b). Other default conditions unless otherwise noted are 6 mM $HAuCl_4$ (Figure 1a), 20 mg mL^{-1} trypsin, pH 12, 37 °C, and 6 h (Figure 1b).

of gold nanoparticles superstructures like double helices or hybrid spheres. Similar to the synthesized peptides, some natural proteins also contains Au binding (and reducing) amino acids. Particularly, they have unique spatial architectures and confined cavities (or cages), which can also direct the gold nanoparticles growth.[16] In this respect, ferritin is a classical protein with cages for synthesis of size-controlled inorganic nanoparticles.[17] For gold nanoparticle synthesis, Colombo et al.[18] reported a novel synthesis of GNPs using spaBC3 (B-domain variant of protein A, 75 kDa) as a capping agent, resulting in gold nanoparticles suitable for functionalization with human IgGs. In addition, many other proteins, such as fibroin,[19] enzyme R-amylase[20] had also been used as templates to direct the synthesis of gold nanoparticles.[21]

Recently, some specific proteins have been proposed to synthesize fluorescent gold nanoclusters consisting of several to tens of atoms. A classic example is the use of bovine serum albumin (BSA) to sequester and reduce Au precursors in situ.[22] The as-prepared GNCs consist of 25 gold atoms with red emission at 640 nm (the quantum yield is ∼6%). Up to now, only several proteins have been reported for GNCs synthesis, including lysozyme type VI,[23] lactoferrin,[24] pepsin,[25] horseradish peroxidase,[26] and insulin.[27] These novel GNCs have been successfully applied to bioimaging and biosensing due to their excellent optical properties. Although it was not very clear how these proteins biomineralized the ultra-small GNCs at the molecular level, results suggest that their specific spatial structures, confined inner cages, binding, and reducing abilities play important roles in GNCs formation. Previous studies have demonstrated the protein-assisted synthesis of pure GNPs or GNCs nanostructures. However, thus far, there is no report on the design of a GNPs−GNCs nanocomposite. Surface modification of GNPs with GNCs may enable formation of this hybrid gold nanostructure with novel or different functions.

Herein, we report an innovative one-pot synthesis of a gold nanoparticles-trypsins-nanoclusters (GNPs-Trys-GNCs) nanocomposite by using trypsin as linking and reducing agents. The trypsin molecule contains 7 cysteines (with the −SH group) and 10 tyrosines (with the phenolic group). These specific amino acids had been shown to bind and reduce $AuCl_4^-$ ions in alkaline pH (above the pK_a).[22,28] The binding and reducing ability of trypsin molecules, combined with the electrostatic interactions under alkaline conditions, enable them to control the GNPs nucleation and growth, resulting in protein-stabilized GNPs. Meanwhile, the inner space of the individual trypsin molecule can provide an effective scaffold for the formation of GNCs. The resulting GNCs-embedded trypsin, similar to its original state, can bind to the surface of GNPs and thus form a GNPs-Trys-GNCs nanocomposite. This specific structure was examined by UV−vis spectroscopy, transmission electron microscopy (TEM), and size exclusion chromatography (SEC) in this work. Furthermore, heavy metal ion Pb^{2+} was chosen as the model to characterize the different optical properties from the GNPs alone, as well as to demonstrate its potential applications in heavy metal ion sensing and elimination.

EXPERIMENTAL SECTION

Materials. Gold(III) chloride trihydrate ($HAuCl_4{\cdot}3H_2O$) powder and N_α-benzoyl-DL-arginine 4-nitroanilide hydrochloride (BApNA) were purchased from Aladdin Reagent Corporation (Shanghai, China). Trypsin from bovine pancreas was purchased from Beijing Probe Bioscience Corporation (Beijin, China). The other reagents were of the highest grades available commercially. All glasswares were soaked in aqua regia overnight and then rinsed with distilled Milli-Q (Millipore Corp.) water three times before use.

Synthesis of GNPs-Trys-GNCs Nanocomposite. Fresh chloroauric acid and trypsin stock solutions were prepared by dissolving them in deionized water at a concentration of 200 mM and 20 mg mL^{-1}, respectively (prepared just before use). In a typical experiment, 4 mM of $HAuCl_4$ solution (diluted from 200 mM stock solution) was rapidly added into trypsin solution (20 mg mL^{-1}) with vigorous shaking at room temperature. After 3 min, the pH of the solution was tuned to 12 by adding an appropriate amount of 1 M NaOH. The resulting mixture was transferred to a water bath shaker at 37 °C and 200 rpm and then incubated for an appropriate time (from 0 to 510 min, as indicated in Figure 1a). The synthetic gold nanocomposite was analyzed immediately or placed in a 4 °C refrigerator.

Characterization of GNPs-Trys-GNCs Nanocomposite. During the gold nanocomposite synthesis process, aliquot samples of the reaction mixture were taken out at different time points for UV−vis measurements in the wavelength range from 200 to 900 nm. The characteristic absorption peak of the gold nanocomposite was recorded with increasing time until no change was observed. High resolution transmission electron microscopy (HRTEM) was performed on a JEM-2100F field emission transmission electron microscope (JEOL, Tokyo, Japan) at an accelerating voltage of 200 kV. To prepare samples for TEM analysis, the gold nanocomposite solution was diluted and dispersed ultrasonically with deionized water. Then a drop of the resulting solution was deposited on the carbon-coated copper mesh and air-dried at room temperature. Size exclusion chromatography (SEC) analysis was performed with a Hiload Sephadex 75 column in the ÄKTA purifier chromatography system (GE Healthcare, USA) by using deionized water as mobile phase (1.0 mL min^{-1}). The protein (trypsin) and gold nanocomposite were monitored by

measuring the absorption at 280 and 520 nm simultaneously with elution time.

Determination of Trypsin Activity. The enzymatic activity of raw trypsins and gold nanocomposite (GNPs-Trys-GNCs) were measured using BApNA as the standard chromogenic substrate.[29] A total of 21.7 mg BApNA was dissolved in 5 mL DMSO and then diluted with Tris-HCl buffer (50 mM, pH 8.0) containing 10 mM $CaCl_2$ to a final concentration of 50 mM. Thirty microliters of raw trypsin solution (20 mg mL^{-1}) or gold nanocomposite solution was mixed with 2.97 mL BApNA solution (50 mM, pH 8.0) at 25 °C. The product (p-nitroaniline) from BApNA hydrolysis was measured by monitoring the change of absorbance at 410 nm with an UV−vis spectrophotometer every 30 s for 10 min. The activity of trypsin (U) is calculated with the following equation: U = A(410)/min ×1000 × 3/8800/mg enzyme, where 8800 is the extinction coefficient of p-nitroaniline, and 3 is the total volume of reaction mixture.

Interaction between GNPs-Trys-GNCs Nanocomposite and Pb^{2+} Ions. Lead nitrate ($Pb(NO_3)_2$) solution with different concentrations was prepared by dissolving lead nitrate powder in ddH_2O. Then 100 μL of $Pb(NO_3)_2$ solution was added into 2.9 mL 6.5 nM of gold nanocomposite solution with vigorous shaking. After incubation in the air shaker (150 rpm, 25 °C) for 20 min, the mixture solution was centrifuged at 12000 rpm. The resulting supernatant was analyzed by UV−vis spectroscopy immediately.

RESULTS AND DISCUSSION

To monitor the formation of gold nanostructures, UV−vis spectroscopy was used to characterize the resulting samples in real-time, as shown in Figure 1a. UV−vis absorption spectra exhibit a surface plasmon resonance (SPR) peak at 520 nm that increase gradually in intensity over time. The results suggest the formation of stable gold nanoparticles solution due to the reducing and capping abilities of the trypsin molecules. Similar to other proteins or peptides, the specific amino acids in trypsin, such as cysteines and tyrosines, should play important roles in GNPs formation.[18,30] These amino acids interact with $AuCl_4^-$ ions to trigger the nucleation and growth of GNPs in alkaline pH.

Previous studies have shown that the amount of $HAuCl_4$ in the reaction system is an important factor affecting the size and shape of the formed gold nanostructures.[31−33] Herein, we also investigated the effect of the $AuCl_4^-$ ion concentration on the growth of gold nanoparticles. As shown in Figure 1b, the intensity of the SPR peak in UV−vis spectra increased obviously with increasing the $AuCl_4^-$ ion concentration from 4 to 10 mM, while there was no change in their corresponding wavelength located at 520 nm. A number of studies have suggested that the SPR frequency of metal nanoparticles closely depends on their size, shape, and aggregation state.[10,34−37] Spherical GNPs with a diameter of ∼20 nm possess an intense SPR absorption band centered at 520 nm. The SPR band will red-shift to a longer wavelength with an increasing diameter in the range of 1 to 100 nm. In this work, UV−vis results (Figure 1b) suggest that the generated GNPs under different $AuCl_4^-$ concentrations are spherical shape with a similar size.

To gain a direct insight into the microstructures of gold nanoparticles, transmission electron microscopy (TEM) was employed to observe the morphologies of the resulting samples. As shown in Figure 2a and c, we can clearly observe gold nanoparticles with spherical shapes. From the respective histograms (inset images), the as-prepared GNPs revealed good size uniformity. The diameters of GNPs, upon averaging over 200 particles, was calculated to be ∼5.5 nm. At different $AuCl_4^-$ concentrations, the GNPs represent similar size distribution and average diameter (Figure 2a, c and Figure S1, Supporting Information), which is in agreement with the UV−vis optical absorption spectrum (Figure 1b). Interestingly, in high resolution TEM images (Figure 2b, d and Figure S2, Supporting Information), we see ultra-small spherical gold nanoclusters around the GNPs. These GNCs are approximately 1 nm in diameter, and some of them are tightly adhered to the GNPs surfaces. Combined with the results from previous studies,[22,24] we speculate that specific amino acid residues in trypsin, such as thiols and phenolic groups, could bind and reduce $AuCl_4^-$ ions, leading to the formation of GNCs in the inner cavity of the trypsin. Meanwhile, the free trypsins and the GNCs-embedded trypsins could interact with $AuCl_4^-$ ions as capping (or binding) and reducing agents to control the growth of GNPs. For individual GNPs, free trypsins or GNCs-embedded trypsins or both of them were bound onto the GNPs surfaces, resulting in a stable GNPs-GNCs solution.

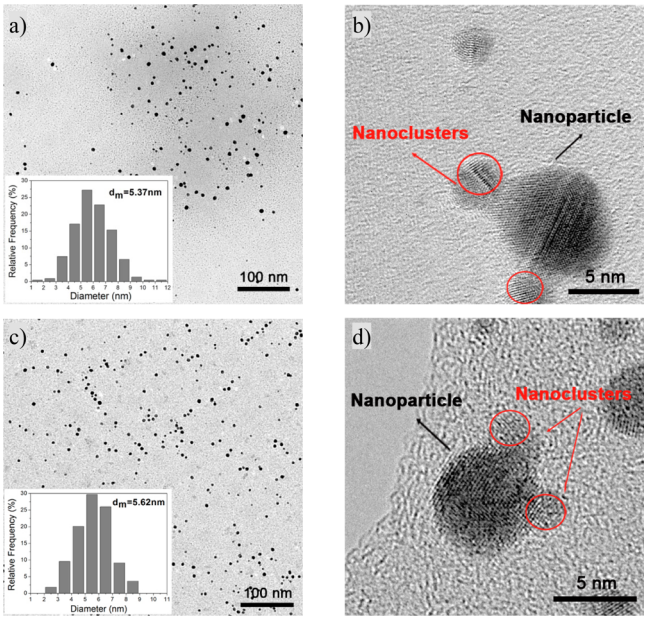

Figure 2. TEM images of gold composite nanostructures formed under different $HAuCl_4$ concentrations: (a, b) 4 mM; (c, d) 8 mM. Other default conditions unless otherwise noted are 20 mg mL^{-1} trypsin, pH 12.0, 37 °C, and 6 h. Inset images are the size distributions of GNPs through statical analysis of 200 particles. GNPs have average diameters of about 5.5 nm, while the GNCs diameters are about 1 nm.

To confirm the structure of GNPs-GNCs in aqueous solution, we employed size exclusion chromatography (SEC) to separate the gold nanostructures with different sizes. Because of the protein capping layer on the gold surface, the gold nanostructures are compatible with standard liquid chromatography media used in protein purification. Similar results have been demonstrated by Lévy et al.,[38] who used SEC with Sephadex G25 to separate the peptide-capped gold nanoparticles from the excess peptide and citrate. In this study, the SEC was operated on Sephadex 75 column using deionized water as the mobile phase. As shown in Figure 3, SEC chromatogram recorded at 520 nm (red line) has an intense peak, which corresponds to the larger GNPs. In SEC chromatogram at 280 nm (black line, Figure 3), as characteristic of proteins, three peaks appeared at different retention times. The first peak at ∼44 min, the same as that of the gold nanoparticles, corresponds to trypsins that linked to the GNPs surfaces. However, whether these trypsins contain GNCs in the inner space needs further confirmation. For the other two

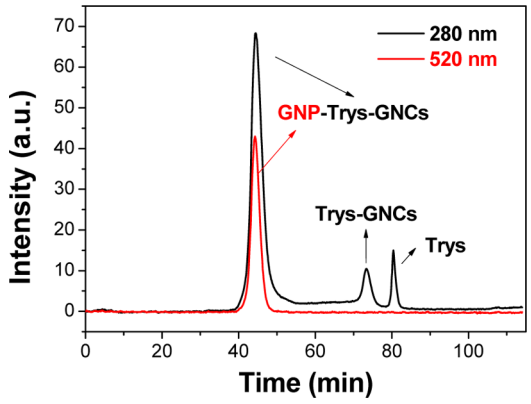

Figure 3. Size-exclusion chromatography (SEC) of the as-prepared samples. Gold nanostructures synthesis conditions: 6 mM $HAuCl_4$, 20 mg mL^{-1} trypsin, pH 12, 37 °C, and 6 h. Absorbance at wavelength 280 nm (characteristic of protein) and at 520 nm (characteristic of GNPs) was recorded simultaneously with increasing elution time.

peaks, we speculate they should correspond to trypsins-GNCs and free trypsins, respectively.

After SEC separation, the first peak of eluent was characterized by TEM (Figure 4). Highly uniform GNPs with

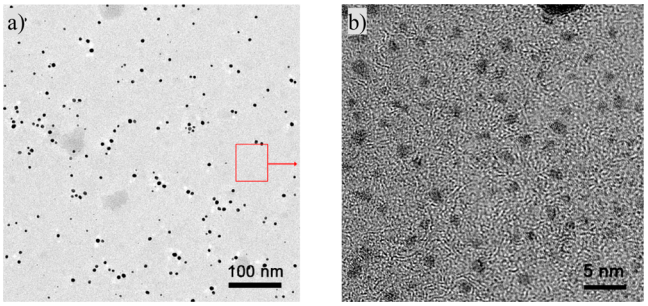

Figure 4. (a) TEM image of the first elution peak, which corresponds to the gold nanocomposite, GNPs-Trys-GNCs. (b) HRTEM image of Trys-GNCs from a typical zone in panel (a) (red-labeled).

a diameter of ~5.5 nm was shown in Figure 4a. The HRTEM image (Figure 4b) shows a typical zone in Figure 5a, from which we can see that there are a large number of ultra-small GNCs. Combined with the SEC analysis, the TEM results of

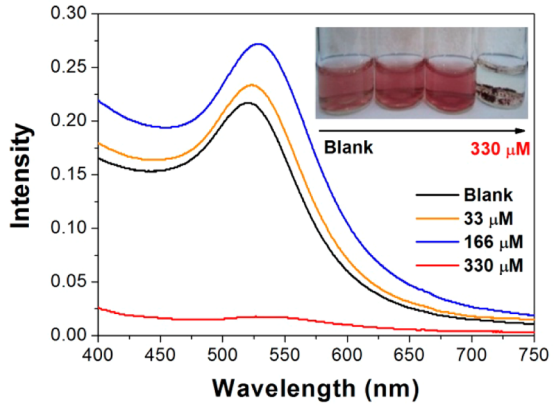

Figure 5. UV–vis spectra of gold composite nanostructures after interacting with Pb^{2+} ions with different concentrations from 0 μM (blank) to 330 μM. The inset image is the corresponding real pictures.

peak 1 indicate that the GNPs are capped and stabilized with GNCs-embedded trypsins (Trys-GNCs), forming a gold nanoparticles-trypsins-nanoclusters (GNPs-Trys-GNCs) nanocomposite. Before TEM observation, dilution and ultrasonic treatment are required to disperse the GNPs for sample preparation. As a result, some Trys-GNCs dropped from the surface of GNPs, leading to dispersed Trys-GNCs in the HRTEM image (Figure 4b). The samples from the other two elution peaks (Figure 3, black line) were also analysized by HRTEM, and the results suggested that the second and third peaks correspond to the Trys-GNCs (Figure S3, Supporting Information) and free trypsins (data not shown), respectively. The above SEC and TEM results were in good agreement with our previous speculation.

Furthermore, we tested the enzymatic activity of trypsin in a gold nanocomposite using BApNA as the substrate. The change of absorbance at 410 nm, which is characteristic of p-nitroaniline from BApNA hydrolysis, with the reaction time is shown in Figure S4 of the Supporting Information. The results indicate that there is no product (p-nitroaniline) generated when using typsins in GNPs-Trys-GNCs. After the synthesis of the gold nanocomposite, trypsin, as the linking and reducing agents, losts its activity completely. The inactivation of trypsins may be attributed to the redox reaction of specific amino acids in trypsin, the thiol–Au interaction, and the high pH value.

Scheme 1 illustrates a possible mechanism for the formation of the GNPs-Try-GNCs nanocomposite. First, $AuCl_4^{-1}$ ions

Scheme 1. Preparation of GNPs-Trys-GNCs (gold nanoparticles-trypsins-nanoclusters) Composite Nanostructures by Using Trypsin As Linking and Reducing Agents under Basic Conditions at 37 °C[a]

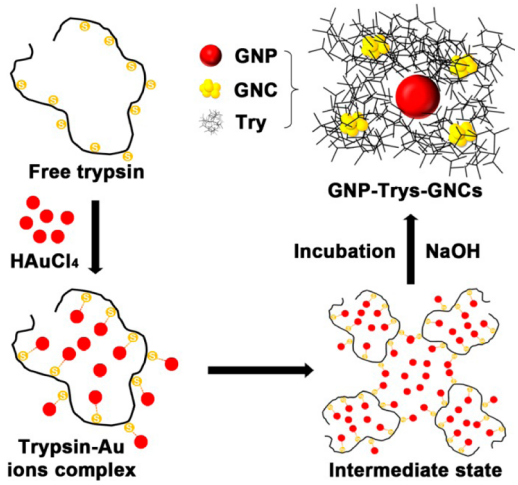

[a]Because of the structural difference between the original trypsin (free trypsin) and GNCs-embedded trypsins, we use two symbols to represent them in this scheme.

were added to a trypsin solution under violent shaking conditions, and some of them entered the inner space of the trypsins. Trypsin has rich amino acids with thiol groups, which strongly bind the $AuCl_4^-$ ions, forming a trypsin–Au ion complex. After adjusting the pH to 12 by adding NaOH solution, the reduction function of the amino acid residues was activated to trigger the nucleation and growth of the GNPs in the scaffolds between trypsin molecules. Meanwhile, the internal spaces of trypsins might work as templates to produce

smaller GNCs, leading to the formation of a GNPs-Trys-GNCs nanocomposite.

GNPs have been used extensively for heavy metal ion sensing, such as Hg^{2+}, Pb^{2+}, and Cu^{2+}, based on the distance-dependent optical property of the GNPs.[39−41] In this work, the heavy metal ion Pb^{2+} was chosen as the model to characterize the different optical properties of the GNPs-Trys-GNCs nanocomposite from the GNPs alone. Figure 5 shows UV−vis spectra of the GNPs-Trys-GNCs solution after interacting with different concentrations of Pb^{2+} ions. When the concentration of Pb^{2+} ions is low, 33 and 166 μM, the color of the solution stayed red while the intensity of the SPR peak representative of the GNPs moved up and red-shifted slightly. However, when the concentration of the Pb^{2+} ions increased to 330 μM, the SPR peak in the UV−vis spectrum disappeared, accompanied by precipitates in the solution, leaving the supernatant clear and colorless. This is obviously different from the results in previous studies using pure GNPs. In these works, the GNPs solutions are red colored with a SPR peak around 520 nm. After changing the charge state[42] or removing the protective layer[39] on the surfaces of the GNPs by adding some specific agents like heavy metal ions, GNPs aggregation occurred, leading to purple or blue solution and a red-shifted peak (e.g., 700 nm) in the UV−vis spectra. The reverse process of anti-aggregation of GNPs has also been utilized to detect Hg^{2+} ions[43] and small molecules like glutathione[41] and cocaine.[40] In our work, the UV−vis result shows that the SPR peak increased in intensity while no obvious red-shift of peak position was observed. This should be attributed to the unique structure of the GNPs-Trys-GNCs nanocomposite.

To understand the interaction between the GNPs-Trys-GNCs nanocomposite and Pb^{2+} ions, a dynamic light scattering (DLS) measurement was performed in this study. As shown in Figure 6, increasing the concentration of Pb^{2+} ions to 25.8 μM,

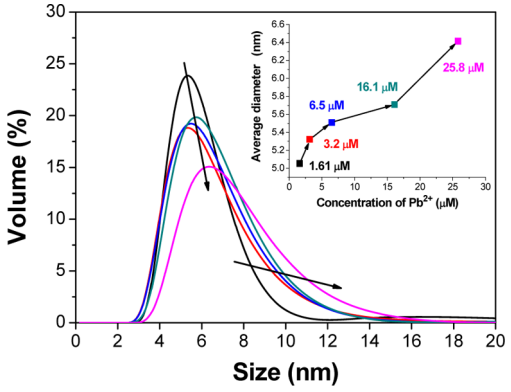

Figure 6. DLS analysis of the hydrodynamic diameter of gold nanostructures with an increasing concentration of Pb^{2+} ions from 1.6 to 25.8 μM. The inset image is the average diameter (D_m) of the gold nanostructures as a function of Pb^{2+} ion concentrations (Color of lines (−) and symbols (■) are matchable at the same Pb^{2+} concentrations).

the hydrodynamic size increased apparently along with a broadened size distribution. The inset image shows the average hydrodynamic diameter D_m gradually increases with the content of lead ions. The DLS results suggest that Pb^{2+} ions can act as joints between GNPs-Trys-GNCs and free Trys-GNCs or trypsins in the solution, leading to an increased size of the GNPs-Trys-GNCs nanocomposite.

Heavy metal ions can influence the microenvironment of the surface of gold nanoparticles through chelating with ligands molecules, such as L-cysteine,[44] and trypsin in our work. When adding heavy metal ions, aggregation of gold nanoparticles occurred due to binding with chelating ligands.[44,45] One Pb^{2+} ion may bind two or more trypsin molecules to the surface of the GNPs-Trys-GNCs nanocomposite, and the small quantity of Trys-GNCs and trypsins disappeared rapidly when increasing the amount of Pb^{2+} ions. The richer the Pb^{2+} ions in the solution, the more and bigger the chelation networks became, and gradually, precipitation occurred. Scanning electron microscope (SEM) equipped with an energy-dispersive X-ray (EDX) detector was utilized to characterize the precipitate produced by the chelating process (Figure S5, Supporting Information). The EDX analysis shows a rather high content of Pb in precipitate that verified the chelation function of Pb^{2+} during the whole process.

The specific mechanism for the above-mentioned phenomenon is illustrated in Scheme 2. We have demonstrated that the

Scheme 2. Proposed Process of Interaction between Gold Nanostructures and Pb^{2+} Ions

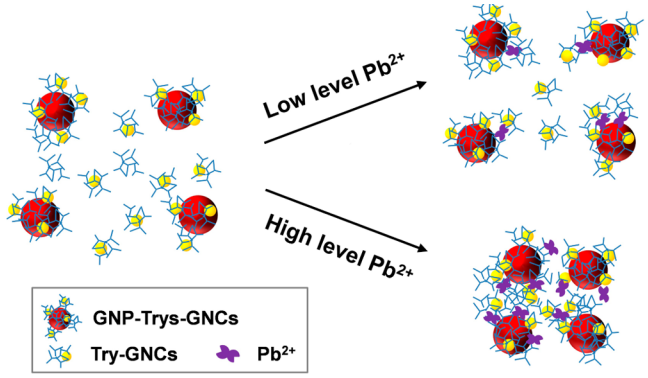

main component in the solution is the GNPs-Trys-GNCs nanocomposite; the others are small amounts of dissociate Trys-GNCs and free trypsins (Figure 3). In a particular content range (low-level Pb^{2+}) , Pb^{2+} ions can change the microenvironment of the GNPs-Trys-GNCs surfaces by electrostatic adsorption or complexing action, resulting in the binding of Try-GNCs and free trypsins. The increased size of the GNPs-Trys-GNCs nanostructure (Figure 6) can probably lead to a slight red-shift of the SPR peak (Figure 5), while the increased SPR intensity may be attributed to the change in the Trys-GNCs content on the GNPs-Trys-GNCs surface. When the concentration of Pb^{2+} ions was 330 μM, it was high enough to induce aggregation of the GNPs-Trys-GNCs and Trys-GNCs accompanied by the formation of precipitate and the disappearance of the SPR peak. This property enables formation of the GNPs-Trys-GNCs nanocomposite with the function of heavy metal ions elimination.

On the basis of the change in SPR intensity under different concentrations of Pb^{2+} ions, we furtherly developed a label-free colorimetric method for detection of Pb^{2+} ions. As shown in Figure 7, the intensity of the SPR absorption at 520 nm is linearly related to the concentration of Pb^{2+} ions within the concentration range investigated (from 1.6 to 32.3 μM, R^2 = 0.9731). In previous studies, the absorption ratio (e.g., $A_{670\ nm}/A_{520\ nm}$, $A_{700\ nm}/A_{518\ nm}$) was often used to express the molar ratio of aggregated and dispersed pure GNPs corresponding to

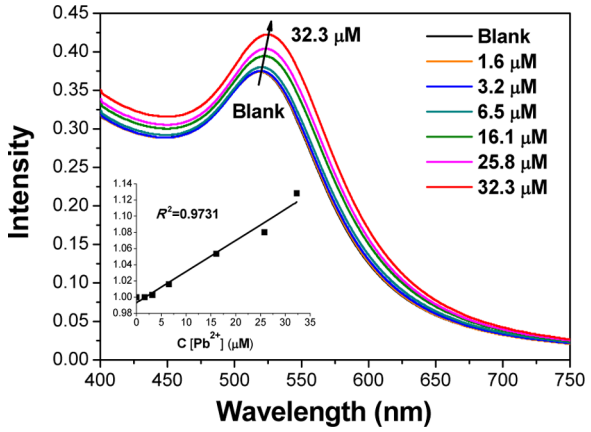

Figure 7. Colorimetric analysis of the interaction between gold composite nanostructures and Pb^{2+} ions with low concentrations. The inset image is the change in the relative absorption value (A/A_0) at 520 nm.

heavy metal ions concentrations.[42,44] In our method, the SPR intensity was directly used to reflect the change in concentrations of Pb^{2+} ions due to the unique optical properties of the GNPs-Trys-GNCs nanocomposite. The results indicated the high potential of this GNPs-Trys-GNCs nanocomposite for colorimetric detection of Pb^{2+} ions in aqueous solutions.

CONCLUSION

In conclusion, we have reported a green synthesis of a novel GNPs-Trys-GNCs nanocomposite using trypsin as the reducing and stabilizing agents. In the gold nanocomposite, GNCs-embedded trypsins (Trys-GNCs) are attached to the surface of GNPs via a ligand, e.g., thiolate ligand−Au interaction. SEC and TEM results provide consistent evidence in support of this composite structure. The as-prepared GNPs-Trys-GNCs nanocomposite contains GNPs with average diameters of 5.5 nm and the GNCs (about 1 nm)-embedded trypsins. The trypsin molecule has rich amino acids with thiol (e.g., cysteine) and phenolic groups (e.g., tyrosine), which can strongly bind and reduce the $AuCl_4^-$ ions, forming trypsin-stabilized gold nanostructures. The binding and reducing abilities, combined with the unique spatial structures, enable trypsins to direct the synthesis of GNPs and GNCs simultaneously. Furthermore, the interaction between gold nanocomposites and Pb^{2+} ions show a different behavior from that of pure GNPs alone. In our work, low-level Pb^{2+} ions can induce an increase in SPR intensity and a slight red-shift of SPR peak, which may attribute to the change of Trys-GNCs content on the GNPs-Trys-GNCs surface and the increased size of gold nanocomposite. For pure GNPs solutions in previous studies, however, the aggregation of GNPs occurred in the presence of heavy metal ions, leading to a decrease in SPR intensity and a new peak in the longer wavelength (e.g., 700 nm) in the UV−vis spectra. On the basis of this unique optical behavior, we developed a label-free colorimetric method for detection of Pb^{2+} ions in aqueous solutions. This method shows a good linear relationship between SPR intensity and the concentration of Pb^{2+} over the range of 1.6−32.3 μM (R^2 = 0.9731). The results indicated that the GNPs-Trys-GNCs nanocomposite is very promising for colorimetric detection of Pb^{2+} ions. Generally, we believe that this synthesis protocol of gold nanocomposite can be applied to other proteins and metals with different functions.

ASSOCIATED CONTENT

Supporting Information

Data as mentioned in the text. This material is available free of charge via the Internet at http://pubs.acs.org.

AUTHOR INFORMATION

Corresponding Authors

* E-mail: tjuhrl@tju.edu.cn (R.H.). Tel: +86 22 27407799. Fax: +86 22 27407599.
* E-mail: surx@tju.edu.cn (R.S.). Tel: +86 22 27407799. Fax: +86 22 27407599.

Notes

The authors declare no competing financial interest.

ACKNOWLEDGMENTS

This work was supported by the Natural Science Foundation of China (20806057, 21276192, 31071509, and 21306134), Ministry of Science and Technology of China (2012AA06A303, 2012YQ090194, and 2012BAD29B05), and Ministry of Education (B06006 and NCET-11-0372).

REFERENCES

(1) Guo, S.; Wang, E. Noble metal nanomaterials: Controllable synthesis and application in fuel cells and analytical sensors. *Nano Today* **2011**, *6* (3), 240−264.
(2) Reilly, S. M.; Krick, T.; Dass, A. Surfactant-free synthesis of ultrasmall gold nanoclusters. *J. Phys. Chem. C* **2009**, *114* (2), 741−745.
(3) Das, A.; Li, T.; Nobusada, K.; Zeng, Q.; Rosi, N. L.; Jin, R. Total structure and optical properties of a phosphine/thiolate-protected Au_{24} nanocluster. *J. Am. Chem. Soc.* **2012**, *134* (50), 20286−20289.
(4) Wu, Z.; Wang, M.; Yang, J.; Zheng, X.; Cai, W.; Meng, G.; Qian, H.; Wang, H.; Jin, R. Well-defined nanoclusters as fluorescent nanosensors: A case study on $Au_{25}(SG)_{18}$. *Small* **2012**, *8* (13), 2028−2035.
(5) Qian, H.; Zhu, M.; Wu, Z.; Jin, R. Quantum sized gold nanoclusters with atomic precision. *Acc. Chem. Res.* **2012**, *45* (9), 1470−1479.
(6) Lin, C. A. J.; Lee, C. H.; Hsieh, J. T.; Wang, H. H.; Li, J. K.; Shen, J. L.; Chan, W. H.; Yeh, H. I.; Chang, W. H. Review: Synthesis of fluorescent metallic nanoclusters toward biomedical application: recent progress and present challenges. *J. Med. Biol. Eng.* **2009**, *29* (6), 276−283.
(7) Arvizo, R. R.; Bhattacharyya, S.; Kudgus, R. A.; Giri, K.; Bhattacharya, R.; Mukherjee, P. Intrinsic therapeutic applications of noble metal nanoparticles: past, present and future. *Chem. Soc. Rev.* **2012**, *41* (7), 2943−2970.
(8) Moyano, D. F.; Rotello, V. M. Nano meets biology: Structure and function at the nanoparticle interface. *Langmuir* **2011**, *27* (17), 10376−10385.
(9) Mout, R.; Moyano, D. F.; Rana, S.; Rotello, V. M. Surface functionalization of nanoparticles for nanomedicine. *Chem. Soc. Rev.* **2012**, *41* (7), 2539−2544.
(10) Slocik, J. M.; Stone, M. O.; Naik, R. R. Synthesis of gold nanoparticles using multifunctional peptides. *Small* **2005**, *1* (11), 1048−1052.
(11) Slocik, J. M.; Naik, R. R.; Stone, M. O.; Wright, D. W. Viral templates for gold nanoparticle synthesis. *J. Mater. Chem.* **2005**, *15* (7), 749−753.
(12) Shao, Y.; Jin, Y.; Dong, S. Synthesis of gold nanoplates by aspartate reduction of gold chloride. *Chem. Commun.* **2004**, *9*, 1104−1105.
(13) Chen, C. L.; Zhang, P. J.; Rosi, N. L. A new peptide-based method for the design and synthesis of nanoparticle superstructures: Construction of highly ordered gold nanoparticle double helices. *J. Am. Chem. Soc.* **2008**, *130* (41), 13555−13557.

(14) Chen, C. L.; Rosi, N. L. Preparation of unique 1-D nanoparticle superstructures and tailoring their structural features. *J. Am. Chem. Soc.* **2010**, *132* (20), 6902−6903.
(15) Kim, J.; Sadowsky, M. J.; Hur, H.-G. Simultaneous synthesis of temperature-tunable peptide and gold nanoparticle hybrid spheres. *Biomacromolecules* **2011**, *12* (7), 2518−2523.
(16) Crookes-Goodson, W. J.; Slocik, J. M.; Naik, R. R. Bio-directed synthesis and assembly of nanomaterials. *Chem. Soc. Rev.* **2008**, *37* (11), 2403−2412.
(17) Uchida, M.; Klem, M. T.; Allen, M.; Suci, P.; Flenniken, M.; Gillitzer, E.; Varpness, Z.; Liepold, L. O.; Young, M.; Douglas, T. Biological containers: Protein cages as multifunctional nanoplatforms. *Adv. Mater.* **2007**, *19* (8), 1025−1042.
(18) Colombo, M.; Mazzucchelli, S.; Collico, V.; Avvakumova, S.; Pandolfi, L.; Corsi, F.; Porta, F.; Prosperi, D. Protein-assisted one-pot synthesis and biofunctionalization of spherical gold nanoparticles for selective targeting of cancer cells. *Angew. Chem.-Int. Edit.* **2012**, *51* (37), 9272−9275.
(19) Zhou, Y.; Chen, W.; Itoh, H.; Naka, K.; Ni, Q.; Yamane, H.; Chujo, Y. Preparation of a novel core-shell nanostructured gold colloid-silk fibroin bioconjugate by the protein redox technique at room temperature. *Chem. Commun.* **2001**, *23*, 2518−2519.
(20) Rangnekar, A.; Sarma, T. K.; Singh, A. K.; Deka, J.; Ramesh, A.; Chattopadhyay, A. Retention of enzymatic activity of α-amylase in the reductive synthesis of gold nanoparticles. *Langmuir* **2007**, *23* (10), 5700−5706.
(21) Dickerson, M. B.; Sandhage, K. H.; Naik, R. R. Protein-and peptide-directed syntheses of inorganic materials. *Chem. Rev.* **2008**, *108* (11), 4935−4978.
(22) Xie, J.; Zheng, Y.; Ying, J. Y. Protein-directed synthesis of highly fluorescent gold nanoclusters. *J. Am. Chem. Soc.* **2009**, *131* (3), 888−889.
(23) Lin, Y. H.; Tseng, W. L. Ultrasensitive sensing of Hg^{2+} and CH_3Hg^+ based on the fluorescence quenching of lysozyme type VI-stabilized gold nanoclusters. *Anal. Chem.* **2010**, *82* (22), 9194−9200.
(24) Xavier, P. L.; Chaudhari, K.; Verma, P. K.; Pal, S. K.; Pradeep, T. Luminescent quantum clusters of gold in transferrin family protein, lactoferrin exhibiting FRET. *Nanoscale* **2010**, *2* (12), 2769−2776.
(25) Kawasaki, H.; Hamaguchi, K.; Osaka, I.; Arakawa, R. pH-dependent synthesis of pepsin-mediated gold nanoclusters with blue green and red fluorescent emission. *Adv. Funct. Mater.* **2011**, *21* (18), 3508−3515.
(26) Wen, F.; Dong, Y. H.; Feng, L.; Wang, S.; Zhang, S. C.; Zhang, X. R. Horseradish peroxidase functionalized fluorescent gold nanoclusters for hydrogen peroxide sensing. *Anal. Chem.* **2011**, *83* (4), 1193−1196.
(27) Liu, C. L.; Wu, H. T.; Hsiao, Y. H.; Lai, C. W.; Shih, C. W.; Peng, Y. K.; Tang, K. C.; Chang, H. W.; Chien, Y. C.; Hsiao, J. K.; Cheng, J. T.; Chou, P. T. Insulin-directed synthesis of fluorescent gold nanoclusters: preservation of insulin bioactivity and versatility in cell imaging. *Angew. Chem., Int. Ed.* **2011**, *50* (31), 7056−7060.
(28) Si, S.; Bhattacharjee, R. R.; Banerjee, A.; Mandal, T. K. A mechanistic and kinetic study of the formation of metal nanoparticles by using synthetic tyrosine-based oligopeptides. *Chem.—Eur. J.* **2006**, *12* (4), 1256−1265.
(29) Hinterwirth, H.; Lindner, W.; Lämmerhofer, M. Bioconjugation of trypsin onto gold nanoparticles: Effect of surface chemistry on bioactivity. *Anal. Chim. Acta* **2012**, *733*, 90−97.
(30) Bhattacharjee, R. R.; Das, A. K.; Haldar, D.; Si, S.; Banerjee, A.; Mandal, T. K. Peptide-assisted synthesis of gold nanoparticles and their self-assembly. *J. Nanosci. Nanotechnol.* **2005**, *5* (7), 1141−1147.
(31) Sánchez-Iglesias, A.; Pastoriza-Santos, I.; Pérez-Juste, J.; Rodríguez-González, B.; García de Abajo, F. J.; Liz-Marzán, L. M. Synthesis and optical properties of gold nanodecahedra with size control. *Adv. Mater.* **2006**, *18* (19), 2529−2534.
(32) Sau, T. K.; Murphy, C. J. Room temperature, high-yield synthesis of multiple shapes of gold nanoparticles in aqueous solution. *J. Am. Chem. Soc.* **2004**, *126* (28), 8648−8649.
(33) Vigderman, L.; Zubarev, E. R. High-yield synthesis of gold nanorods with longitudinal SPR peak greater than 1200 nm using hydroquinone as a reducing agent. *Chem. Mater.* **2013**, *25* (8), 1450−1457.
(34) Slocik, J. M.; Zabinski, J. S.; Phillips, D. M.; Naik, R. R. Colorimetric response of peptide-functionalized gold nanoparticles to metal ions. *Small* **2008**, *4* (5), 548−551.
(35) Sun, Y.; Xia, Y. Gold and silver nanoparticles: A class of chromophores with colors tunable in the range from 400 to 750 nm. *Analyst* **2003**, *128* (6), 686−691.
(36) Shankar, S. S.; Rai, A.; Ankamwar, B.; Singh, A.; Ahmad, A.; Sastry, M. Biological synthesis of triangular gold nanoprisms. *Nat. Mater.* **2004**, *3* (7), 482−488.
(37) Jain, P. K.; El-Sayed, I. H.; El-Sayed, M. A. Au nanoparticles target cancer. *Nano Today* **2007**, *2* (1), 18−29.
(38) Lévy, R.; Thanh, N. T. K.; Doty, R. C.; Hussain, I.; Nichols, R. J.; Schiffrin, D. J.; Brust, M.; Fernig, D. G. Rational and combinatorial design of peptide capping ligands for gold nanoparticles. *J. Am. Chem. Soc.* **2004**, *126* (32), 10076−10084.
(39) Liu, J.; Lu, Y. Fast colorimetric sensing of adenosine and cocaine based on a general sensor design involving aptamers and nanoparticles. *Angew. Chem., Int. Ed.* **2006**, *45* (1), 90−94.
(40) Li, Y.; Wu, P.; Xu, H.; Zhang, H.; Zhong, X. Anti-aggregation of gold nanoparticle-based colorimetric sensor for glutathione with excellent selectivity and sensitivity. *Analyst* **2011**, *136* (1), 196−200.
(41) Chah, S.; Hammond, M. R.; Zare, R. N. Gold nanoparticles as a colorimetric sensor for protein conformational changes. *Chem. Biol.* **2005**, *12* (3), 323−328.
(42) Lou, T.; Chen, L.; Zhang, C.; Kang, Q.; You, H.; Shen, D. A simple and sensitive colorimetric method for detection of mercury ions based on anti-aggregation of gold nanoparticles. *Anal. Methods* **2012**, *4* (2), 488−491.
(43) Mirkin, C. A.; Letsinger, R. L.; Mucic, R. C.; Storhoff, J. J. A DNA-based method for rationally assembling nanoparticles into macroscopic materials. *Nature* **1996**, *382*, 607−609.
(44) Chai, F.; Wang, C. G.; Wang, T. T.; Ma, Z. F.; Su, Z. M. L-cysteine functionalized gold nanoparticles for the colorimetric detection of Hg^{2+} induced by ultraviolet light. *Nanotechnology* **2010**, *21* (2), 025501.
(45) Darbha, G. K.; Singh, A. K.; Rai, U. S.; Yu, E.; Yu, H.; Chandra Ray, P. Selective detection of mercury (II) ion using nonlinear optical properties of gold nanoparticles. *J. Am. Chem. Soc.* **2008**, *130* (25), 8038−8043.